Light diffraction from rough gratings

M. Saillard, E. Popov, L. Tsonev, L. Scandella, and N. Kruse

Two holographic diffraction gratings with very similar parameters, designed for maximum performance in TM polarization, are investigated, their diffraction efficiency measured, an electron microscopic picture of their surface observed, and numerical simulation of light diffraction done with the surface roughness taken into account. It is demonstrated numerically that a small-scale roughness imposed on the grating surface could increase significantly both scattering and absorption from the surface, this influence being greater in the TM case. A very good coincidence between the numerical and experimental data is obtained in TE polarization, whereas in TM polarization only a qualitative agreement exists.

1. Experimental Results

Recently[1] it was demonstrated that in the manufacture of holographic plane gratings, provided the technological process is optimal for obtaining a grating with maximum efficiency in the TM case, the resulting efficiency depends strongly on baking the photoresist before vacuum evaporation of the aluminum reflecting coating. In particular, without the baking, the sum of all the diffracted orders efficiencies hardly exceeds 60%, whereas the same quantity for the correctly manufactured grating (that has undergone several hours of prebaking before aluminization) could reach 86–87%. A typical example of such behavior is presented in Figs. 1 and 2; 2400-line/mm gratings, prepared with (Fig. 1) and without (Fig. 2) prebaking, were measured for the spectral dependence of their efficiencies with laser light. The difference between the two samples is obvious, although the recording conditions are identical.

The result was almost obvious for physicists dealing with vacuum-layer deposition—it is well known that the presence of impurities during the evaporation could damage significantly the layer properties, and surely there are enough impurities that can evaporate from the unbaked photoresist—water and developer vapors, organic compounds, etc. However, from the optical point of view, a natural question arises: By what mechanism could a given damage of the layer lead to a decrease in layer reflectance? There are two possible directions: a change in the optical properties of the layer and a distortion of the layer surface. The first damage is very difficult to determine because it requires independent measurements of the surface complex refractive index. Our aim in this paper is to investigate the second direction, the influence of the surface roughness on the grating performance. In fact, the specific results of Figs. 1 and 2 serve only as an occasion and stimuli for such an investigation. In the previous paper[1] we studied the efficiency behavior of another set of samples, their period being slightly different (2000 lines/mm), but their spectral response is remarkably similar. Indeed the prebaked gratings are very good, with efficiency of more than 80%, and the bad samples, those not baked, could hardly reach 70% in the best case.

Our main background for the hypothesis of the importance of surface roughness for the effect of reduction of reflection is the result of scanning force microscopy (SFM). The measurements reported here were performed with a commercially available microscope (Nanoscope II, Digital Instruments) in ambient air. Rectangular silicon cantilevers with integrated tips were used. The radii of curvature of the tips were specified (manufacturer, Nanoprobe) to ~10 nm. Recently, some of the measurements reported here were reproduced by use of a contamination tip prepared under vacuum in an electron microscope. The scanner was calibrated with standard optical grids with known periodicity. In addition to the

M. Saillard is with the Faculté des Sciences et Techniques de St-Jérôme, Laboratoire d'Optique Electromagnétique, Avenue Escadrille Normandie-Niemen, 13397 Marseille Cedex 20, France. E. Popov and L. Tsonev are with the Institute of Solid State Physics, Boulevard Tzarigradsko Chaussee 72, Sofia 1784, Bulgaria. When this work was performed L. Scandella and N. Kruse were with Technische Chemisches Laboratory, ETH Zentrum, 8092 Zürich, Switzerland. L. Scandella is now with the Paul Scherrer Institut, 5232 Viligen, Switzerland.

Received 10 February 1994; revised manuscript received 7 December 1994.

0003-6935/95/224883-09$06.00/0.

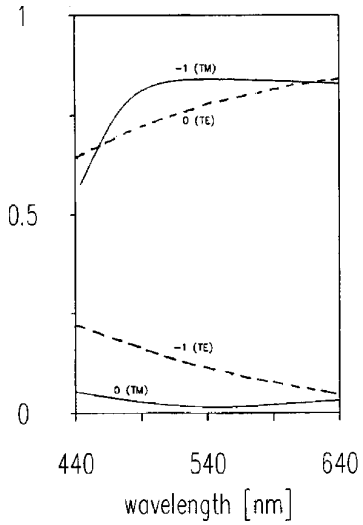

Fig. 1. Spectral dependence of the diffraction efficiency of aluminum holographic grating with 0.41-μm period. Before aluminization the photorest grating was baked for several hours at 120 °C: solid curves, TM polarization; dashed curves, TE polarization.

standard experiment another image was taken, illuminating the sample by an additional light source so that we could visualize the small-scale roughness [see Figs. 3(d) and 4(d)].

A periodicity of 410 ± 10 nm for both gratings was obtained from large-scale SFM measurements and respective fast Fourier transform. Figure 3(b) provides topographic information for the bad grating. Changes in height along the section line are depicted in Fig. 3(a). Smaller structural features become more clearly visible by illumination of the sample surface [Fig. 3(d)]. Single clusters (bubbles) with dimensions of ~60 nm can be clearly identified. However, we must keep in mind that surface structures smaller than the tip radius may be subject to convolution with the tip geometry. Probably the bubbles on the surface are due to the formation of

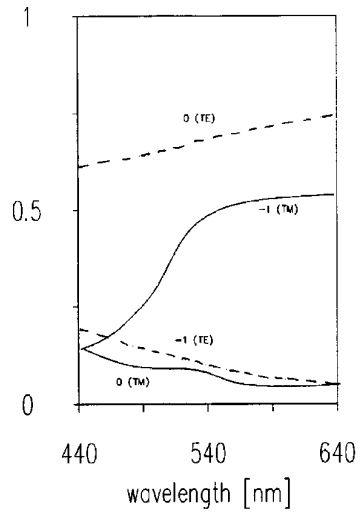

Fig. 2. Same as in Fig. 1. Except for the baking, the aluminization was done directly after development of the photoresist.

Al_2O_3. (The gratings have remained more than one year in air, and the aluminum surface was not covered by any dielectric layer because often such a layer could lead to the appearance of sharp anomalies in the diffraction efficiency.)

Figures 4(b) and 4(d) provide SFM images of the good grating. Compared with Figs. 3(a) and 3(d), the surface is smoother, which is most clearly seen by the trace of the section line. Results from illumination demonstrate that the surface structures are grains with dimensions in the range of 60–100 nm rather than clusters. Figures 3(c) and 4(c) display the spectrum of the section lines and help us to model the profile of the rough gratings with a few geometrical parameters.

Note that the performance of the good grating is not affected, at least at first glance, by the presence of this slight roughness, whereas the greater roughness of the second grating causes, for other reasons, a significant reduction in diffraction efficiency, as demonstrated numerically in Section 2. It is not our aim here to investigate the origin and the nature of the bumps (we are not specialists in this region) but to show that the existence by itself of such roughness can reduce significantly the grating performance.

2. Theoretical and Numerical Study

In this section from numerical experiments we deduce how the efficiencies of the grating are modified when a small-scale, one-dimensional random roughness is superimposed on the periodic profile. With this aim we use a computer code based on a rigorous integral theory devoted to the problem of scattering a finite incident beam by a metallic or dielectric one-dimensional rough surface.[2] We must emphasize that our approach enables us to deal with a particular profile of the surface (deterministic roughness). Provided the sample is large enough, the roughness properties are averaged but there is no assumption including averaging in our model.

Subsections 2.A. and 2.B. are necessary for consistency and completeness, and any grating investigator inexperienced in rough-surface-scattering problems could skip them.

A. Description of the Problem: Notations

The surface is illuminated by a Gaussian incident beam with a mean incidence angle θ_0 and wavelength λ. We denote by F^i the incident electric or magnetic field, depending on whether the beam is TE or TM polarized, respectively:

$$F^i(x, y) = \int_{-\infty}^{+\infty} A(\alpha')\exp(i\alpha' x - i\beta' y)\mathrm{d}\alpha' \qquad (1)$$

with

$$A(\alpha') = A_0 \exp\left[-\frac{(\alpha' - \alpha_0)^2}{2\delta^2}\right], \qquad (2)$$

$$\alpha_0 = k \sin \theta_0, \qquad (3)$$

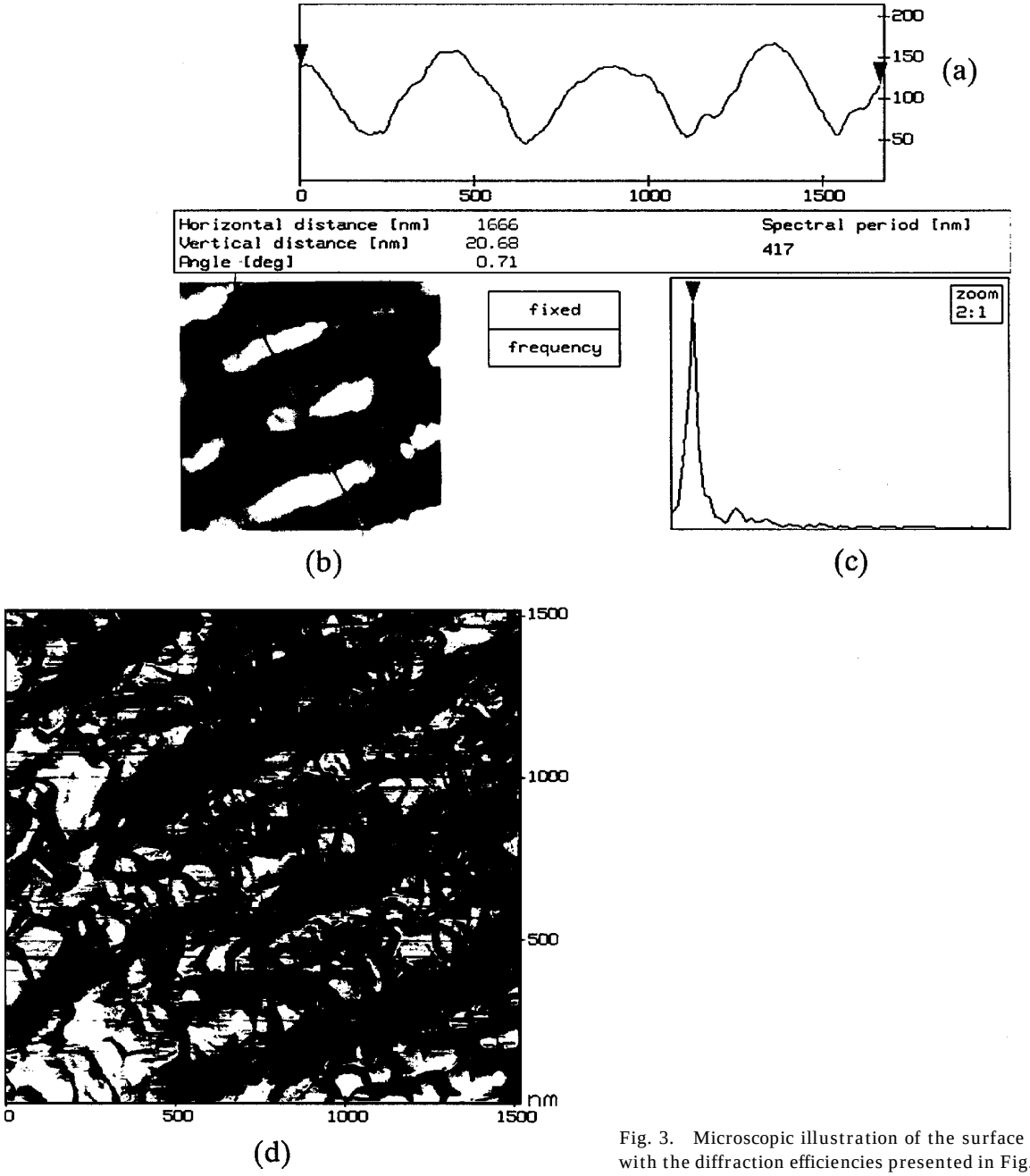

Fig. 3. Microscopic illustration of the surface of the bad grating with the diffraction efficiencies presented in Fig. 2.

$$k = \frac{2\pi}{\lambda}, \tag{4}$$

$$\beta' = (k^2 - \alpha'^2)^{1/2} \text{ or } i(\alpha'^2 - k^2)^{1/2}, \tag{5}$$

where A_0 and δ are complex and real numbers, respectively, characterizing the beam amplitude and width.

From the resolution of the integral equation we obtain the diffracted field at infinity (in y). This field is represented by its Rayleigh expansion:

$$F^d(x, y) = \int_{-\infty}^{+\infty} B(\alpha')\exp(i\alpha' x + i\beta' y)\mathrm{d}\alpha'. \tag{6}$$

As usual, the incident and scattering angles θ_0 and θ' are measured by using the counterclockwise and clockwise conventions, respectively. The intensity of the scattered angle θ is given by

$$I(\theta) = B(\alpha)\overline{B(\alpha)}\cos\theta \tag{7}$$

with

$$\alpha = k \sin\theta, \tag{8}$$

and the overbar denotes complex conjugation.

Because of the beam-simulation method[3] we are

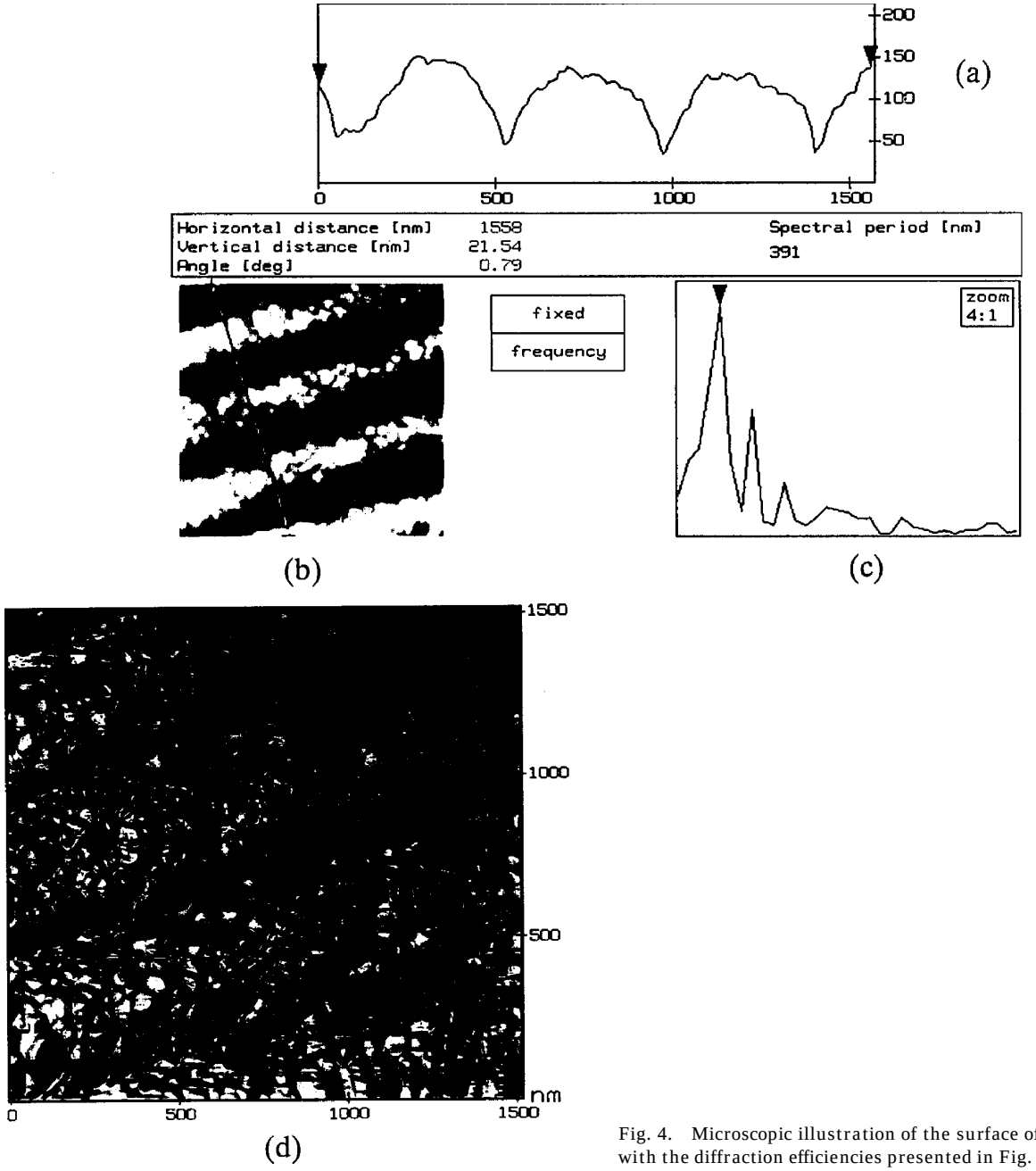

Fig. 4. Microscopic illustration of the surface of the good grating with the diffraction efficiencies presented in Fig. 1.

able to deal with arbitrarily large beams to illuminate a significant number of asperities from a statistical point of view. For example, in the following, the width of the beam along the x axis is $\sim$30 μm when the groove spacing is $d = 0.417$ μm and the mean width of the random asperities is $\sim$0.1 μm. With such parameters a good sampling requires $\sim$3000 points. To avoid solving such a huge linear system, we have divided the incident beam into 17 elementary beams, each 6 μm wide. Because of its finite spatial width, the incident beam has a nonzero angular width and can be considered as a superposition of plane waves with various angles of incidence close to θ_0 [see Eq. (1)]. The same numerical values lead to diffraction orders with a 2-deg angular width. In the resonance domain the number of diffraction orders is small and this is enough to separate them.

Although from an experimental point of view there is no problem (we just measure the intensity of the beam and that of the diffracted order), several questions remain: If the roughness is high or the angular divergence of the incident beam is great, how do we collect all the diffracted energy, how do we take into account the finite size of the detector, etc.? That is why it is better to have, with a good basis, a theoretical answer to the following question: What

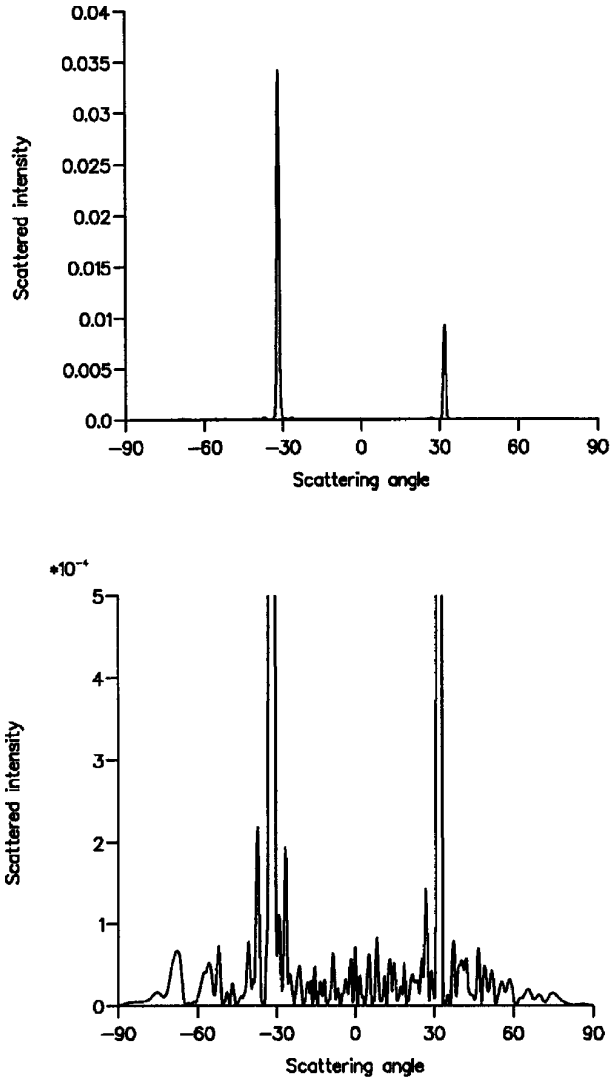

Fig. 5. Top: pattern from the diffraction of a TM-polarized finite beam (width $\approx 50\,\lambda$, $\lambda = 0.44\,\mu$m) by a rough grating modeling the bad grating depicted in Fig. 3. Bottom: enlargement.

is the efficiency of a rough surface, periodic or not, in a given direction when it is illuminated by a finite beam?

B. Generalized Efficiency

In a recent paper,[4] to avoid the shortcomings of the notion of intensity, a generalization of the classical notion of grating efficiency to the arbitrary surface and incident beam has been proposed. It does not depend on the amplitude of the incident beam, it is almost independent of its width, and it reduces to the actual efficiency in the particular case of a periodic surface.

Let us recall now the definition of that generalized efficiency. Considering the amplitudes of the incident and diffracted beams given by Eqs. (1) and (6), we define the new amplitudes $\tilde{A}$ and $\tilde{B}$ as

$$\tilde{A}(\alpha') = A(\alpha')\sqrt{\beta'}, \tag{9}$$

$$\tilde{B}(\alpha') = B(\alpha')\sqrt{\beta'}, \tag{10}$$

and the normalized diffracted amplitude $\mathscr{B}$ by

$$\mathscr{B}(\alpha) = \frac{\langle T_{-\alpha}(\tilde{B}),\, T_{-\alpha_0}(\tilde{A})\rangle}{\langle \tilde{A},\, \tilde{A}\rangle}, \tag{11}$$

where the operator of translation T is defined as

$$T_u[f(\alpha')] = f(\alpha' - u) \tag{12}$$

and the scalar product as

$$\langle f, g\rangle = \int_{-\infty}^{+\infty} f(\alpha')\overline{g}(\alpha')\mathrm{d}\alpha'. \tag{13}$$

Note from Eq. (11) that translating the incident amplitudes and the diffracted ones with $-\alpha_0$ and $-\alpha$, respectively, makes the point in which the amplitude is calculated to coincide with the center of the incident beam. The denominator is simply a normalization factor. Then the efficiency in the direction characterized by α is given by

$$e(\alpha) = \mathscr{B}(\alpha)\,\overline{\mathscr{B}(\alpha)}. \tag{14}$$

When the surface is a grating, $e(\alpha)$ tends to the classical efficiency of the grating provided the incident beam tends toward a plane wave. In the following, the term efficiency denotes $e(\alpha)$.

In Table 1 we can see the values of the efficiencies of the grating that we are dealing with in this paper when the width w of the incident beam is equal to 30 μm; w equal to infinity means that the grating is illuminated by a plane wave. In this case the calculation is achieved with the help of a code devoted to periodic surfaces from Maystre,[5] and its efficiency is well known.

Because there is neither a Rayleigh anomaly nor a Wood anomaly in the neighborhood of the average incidence, the efficiency is not very sensitive to the size of the incident beam. A 50-wavelength width gives a good approximation of the true efficiencies. This accuracy is enough for our purpose.

We must point out that the notion of generalized efficiency is of great interest when the periodicity of the profile is broken by some random roughness. Provided the beamwidth is enough and the roughness is not too high to spoil completely the underlying periodicity, the angular distribution of the scattered field exhibits sharp maxima in specific directions, which are determined by the grating formula. To

Table 1. Efficiencies of a Sinusoidal Grating with Groove Spacing d = 0.417 μm and Height h = 0.14 μm, Illuminated by a TM-Polarized Beam with Incidence Angle θ^i = 49.4° and Wavelength λ = 0.6328 μm

w	50 λ	∞
0-Order efficiency	0.041	0.038
−1-Order efficiency	0.833	0.840

illustrate that, Fig. 5 presents the diffraction pattern of the bad grating modeled according to the procedure described in detail in Subsection 2.C. The parameters are given in the caption of Fig. 8. As is obvious, the diffraction orders clearly appear above the background.

C. Numerical Results: TM Polarization

In this section we calculate the spectral dependence of the efficiencies when the grating is used in the Littrow mount. The width of the incident beam is kept constant and close to 30 μm. It has been checked numerically that a deterministic sample of the surface with such a size represents quite well the statistical properties of the random roughness, which means that the scattering by another sample with the same size shows very similar efficiencies. Here the various samples are statistical realizations of a rough surface with given geometrical parameters (rms height, correlation length).

The incident wavelength is varied in the visible domain from 0.44 to 0.64 μm. At the same time the angle of incidence goes from 31.9° to 49.4°. Knowledge of the actual refractive index is impossible because it depends on too many experimental factors, which explains our choice of bulk aluminum.

To ensure the validity of our results, not only has our code been compared with a rigorous code devoted to gratings (see Subsection 2.B.), but it has also been successfully tested against numerical and experimental data concerned with one-dimensional random rough surfaces.[6] In addition a convergence test is often achieved; i.e., we check the stability of the solution when increasing the number of sampling points and varying the size of the elementary beams. Because of losses in the metal, we cannot test the results against the energy-balance criterion.

When looking at the photographs from the microscope, we can mention that the grooves are sharp and that the curvature is smooth on the top. The average profile is in fact not sinusoidal: When looking at the atomic force microscopy (AFM) figures and at the spectrum of the surface, we see that the important role of the first harmonic [see the profile in Eq. (15)] is obvious. So, we try to describe the profile by the superposition of the fundamental grating (groove spacing d, depth h), its first harmonic ($d' = d/2$, h'), and its random roughness (correlation length τ, rms height σ).

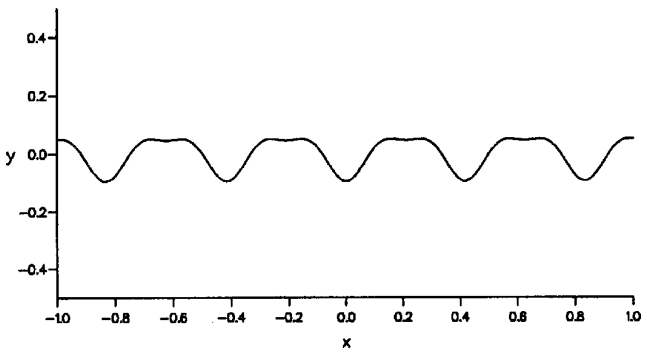

Fig. 6. Profile from the superposition of a sinusoidal grating ($d = 0.417$, $h = 0.14$) and of its first harmonic ($d' = 0.208$, $h' = 0.05$).

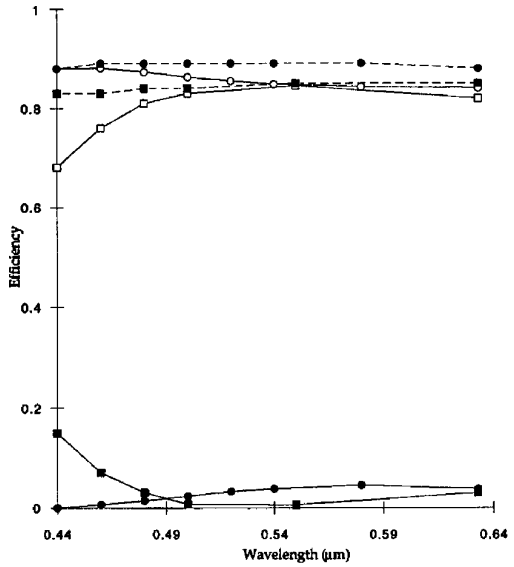

Fig. 7. Comparison of the efficiencies of the sinusoidal grating ($d = 0.417$ μm, $h = 0.14$ μm) with (squares) and without (circles) the superposition of the first harmonic ($d' = 0.208$ μm, $h = 0.05$ μm) for TM polarization: open symbols and solid curve, −1st order; black symbols and solid curve, 0 order; dashed curves, sum of efficiencies.

1. *First Harmonic*

In this section the groove profile is given by

$$y = -h/2 \cos(2\pi x/d) - h'/2 \cos(4\pi x/d). \quad (15)$$

Note that the first harmonic modifies the efficiencies of the perfect sinusoidal grating in a good way with respect to the experimental data for the good grating. For example, for $h = 0.14$ μm, $h' = 0.05$ μm, and $d' = d/2 = 0.208$ μm, the shape of the profile is shown in Fig. 6 and the calculation of the efficiencies leads to the curves plotted in Fig. 7. These parameters were chosen to fit both the profile from the pictures and the efficiencies from measurements of the good grating. This is not accurate, as long as there is a noticeable second harmonic in Fig. 3(c), but the main properties of the surface are satisfactorily described by including the first two harmonics only: The efficiency in the −1st order goes down for blue light and the curvature now agrees with the AFM measurements.

The curves in Fig. 7 show that the superposition of the harmonic increases the absorption and can explain part of the decline of the efficiencies measured on the bad grating.

2. *Random Roughness*

The next step in modeling the profile consists of taking into account the small-scale roughness. Currently, for obvious numerical reasons, we are not able to solve rigorously a scattering problem with arbi-

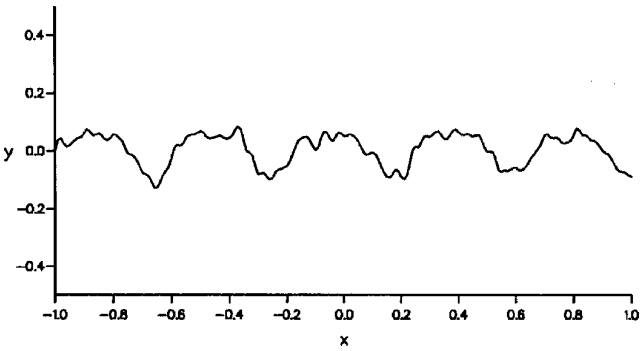

Fig. 8. One-dimensional model for the bad grating, superposition of a sinusoidal grating ($d = 0.417$ μm, $h = 0.14$ μm), of its first harmonic ($d' = 0.208$ μm, $h = 0.05$ μm), and of random roughness ($\tau = 0.021$ μm, $\sigma = 0.012$ μm).

trary two-dimensional random roughness. So, we first assume that the cylindrical symmetry of the grating is not broken.

As long as we do not know the statistics, for simplicity, we assume that the random roughness obeys Gaussian statistics and thus can be described by its rms σ and its correlation length τ.[7] On the basis of the microscopic pictures the geometrical parameters have been estimated. Estimating the size of the small grains to be 0.05–0.06 μm in Figs. 3(d) and 4(d), the corresponding correlation length seems to be $\tau \approx 0.02$ μm. Fitting approximately numerical and experimental data when varying the rms height within the range suggested by verticals cuts such as in Figs. 3(a) and 4(a) led us to choose $\sigma = 0.012$ μm. A short sample of the final one-dimensional surface, which describes the bad grating, is in Fig. 8. In this case the spectral dependence of the efficiencies is given in Fig. 9.

The part of the incident energy that is scattered in the speckle by the random roughness is shown by the difference between the total scattered energy and the sum of the two efficiencies. In addition, we have also plotted in Fig. 9 the sum of the efficiencies of the perfect sinusoidal grating. This permits one to measure the increase in absorption resulting from the harmonic and the random roughness. Now we are able to produce an energy balance: for example, at $\lambda = 0.5$ μm, we find that 6.5% of the energy is in the speckle and that the increase in absorption is 16.5%, which means that a perturbation of the geometrical parameters only can increase the total absorption from 11% to 27.5%, and 34% of the incident energy is not distributed among the diffraction orders.

Although these data are significant, they are smaller than what was expected from the experimental curves. The discrepancy with the experimental data can be explained by the model of the roughness with a cylindrical surface but also, under TM polarization, by the fact that the refractive index of the bad grating is not known. Indeed, for such a range of geometrical parameters, plasmon surface waves are excited on random rough surfaces and may play an important role in the energy balance. Moreover their coupling with the incident wave and their damping rate along the surface strongly depend on the complex index of the metal. Nevertheless, from a qualitative point of view, the superposition of the roughness can explain both the fall of the efficiencies and the shape of the experimental curve, which shows a deeper fall for small wavelengths.

Because the good grating also has some random roughness, studying the influence of a more shallow roughness on the energy balance was interesting. With this aim, we plotted the efficiencies for three

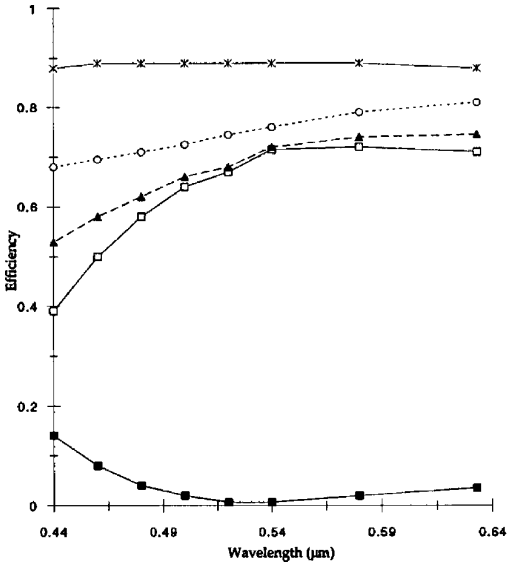

Fig. 9. Efficiencies and energy balance of the rough grating with the profile plotted in Fig. 8 for TM polarization: black squares, 0 order; open squares, −1st order; triangles, sum of efficiencies; circles, total scattered energy; stars, sum of efficiencies of the perfect grating.

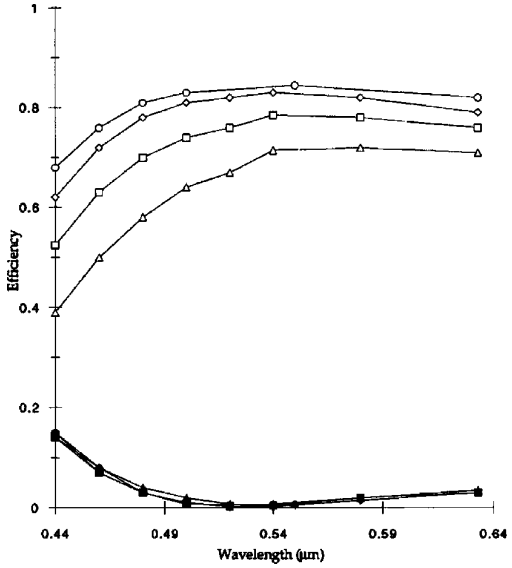

Fig. 10. TM efficiencies of 0 order (black symbols) and −1st order (open symbols) of the rough grating when the rms height of the random component is varied: circles, no random component; diamonds, $\sigma = 0.004$ μm; squares, $\sigma = 0.008$ μm; triangles, $\sigma = 0.012$ μm.

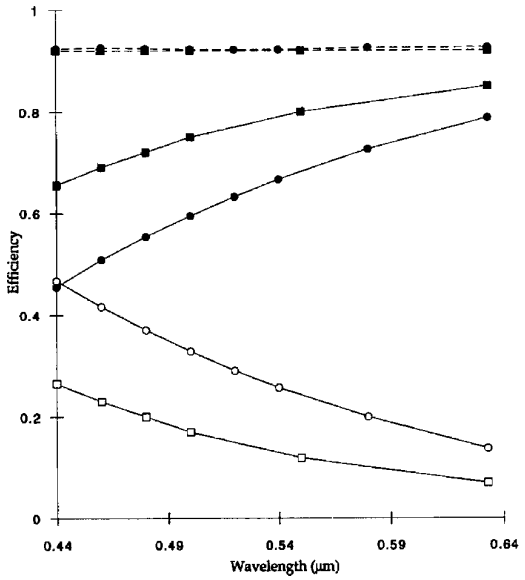

Fig. 11. Same as Fig. 7 for TE polarization.

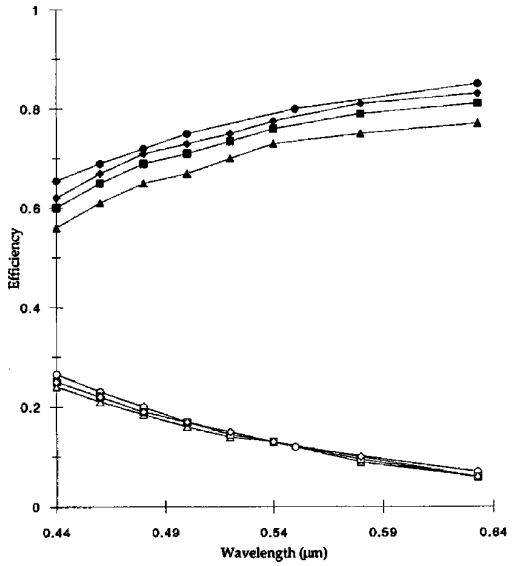

Fig. 13. Same as Fig. 10 for TE polarization.

different values of the rms height (σ = 0.004, 0.008, and 0.012 μm) in Fig. 10. It appears that the fall of the efficiency of the −1st order is almost proportional to the square of the rms height, whereas the 0 order is barely sensitive to the random roughness.

D. Numerical Results: TE Polarization

The same calculations were made in TE polarization, and Figs. 11, 12, and 13 are similar to Figs. 7, 9, and 10, respectively. But the conclusions are different. The main result is the very good agreement with the experimental curves for both the bad grating and the good grating. Note that under TE polarization no surface wave exists and the scattering phenomena are less critical with respect to the complex refractive index of the lower medium.

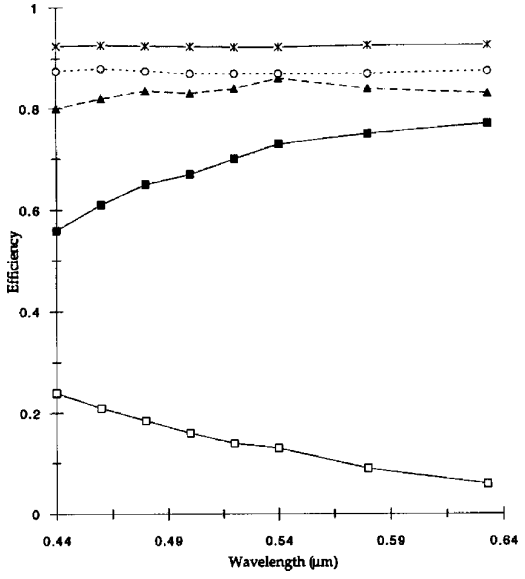

Fig. 12. Same as Fig. 9 for TE polarization.

Figure 11 shows the strong influence of the first harmonic: An important part of the energy moves from the −1st order to the 0 order whatever the incident wavelength, whereas the sum of the efficiencies remains constant. As expected, absorption is not strongly enhanced by the random roughness under TE polarization (three times less than in TM polarization at λ = 0.5 μm; see Fig. 12).

3. Conclusion

This empirical approach of an inverse-scattering problem, mixing deterministic and random rough surfaces, shows the great difficulty with the general problem. In particular, it seems that a description with a few geometrical parameters is not enough. Probably the assumptions about the statistics of the random component are too strong, and surely the assumption that the refractive index is equal to that of the bulk material is not true. In spite of this, the enhancement of absorption and scattering phenomena by the superposition of small-scale random roughness on a metallic grating is clearly shown and agrees qualitatively with experimental work. The absorption is much stronger in the TM case, probably enlarged by surface-wave excitation.

E. Popov and M. Saillard thank the European Communities for their financial support under the BRITE-EURAM Program through contract BRE2-CT92-0288, Flat Optical Antennae.

References and Notes

1. E. Popov, L. Tsonev, and M. Sabeva, "Some technological problems in holographic gratings manufacturing," Opt. Eng. **31,** 2168–2173 (1992).
2. M. Saillard and D. Maystre, "Scattering from metallic and dielectric rough surfaces," J. Opt. Soc. Am. A **7,** 982–990 (1990).
3. M. Saillard and D. Maystre, "Scattering from random rough surfaces: a beam simulation method," J. Opt. **19,** 173–176 (1988).
4. M. Saillard and D. Maystre, "Scattering by quasi-gratings and

space-frequency coupling," J. Opt. Soc. Am. A **10,** 502–508 (1993).

5. D. Maystre, "Rigorous vector theories of diffraction gratings," in *Progress in Optics*, E. Wolf, ed. (Elsevier, New York, 1984), Vol. 21, Chap. 1, p. 3.
6. Experimental and numerical results are in M. E. Knotts, T. R. Michel, and K. O. O'Donnell, "Comparisons of theory and experiment in light scattering from randomly rough surface," in J. Opt. Soc. Am. A **10,** 928–941 (1993). The author's numerical results are in D. Maestra and M. Saillard, "Enhanced backscattering and blazing effects from gratings, quasi-gratings, and randomly rough surfaces," Waves Random Media **4,** 467–485 (1994).
7. M. Saillard, "Etude théorique et numérique de la diffraction de la lumière par des surfaces rugueuses diélectriques et conductrices," Ph.D. dissertation (Université d'Aix-Marseille III, Marseille, 1990).